8. M. L. Michelsen and K. Ostergaard, Chem. Eng. Sci., 25, 583 (1970).
9. K. Ostergaard and M. L. Michelsen, Can. J. Chem. Eng., 47, 108 (1969).
10. E. A. Ebach and R. R. White, Am. Inst. Chem. Eng. J., 4, 161 (1968).
11. P. R. Krishnaswamy and L. W. Shemilt, Can. J. Chem. Eng., 51, 680 (1973).
12. F. E. Head, J. O. Hougen, and R. A. Walsh, in: Proceedings of First International Congress of the International Federation on Automatic Control, Moscow, 1960 [in Russian], Vol. 6, AN SSSR, Moscow (1961), p.207.
13. S. F. Chung and C. Y. Wen, Am. Inst. Chem. Eng. J., 14, 857 (1969).
14. J. R. Hays, W. C. Clements, and T. R. Harris, Am. Inst. Chem. Eng. J., 13, 374 (1967).
15. R. E. Harrison, R. M. Felder, and R. W. Rousseau, Ind. Eng. Chem. Proc. Des. Devel., 13, 389 (1974).
16. T. R. Borrell, G. Muratet, and H. Angelino, Chem. Eng. Sci., 29, 1315 (1974).
17. M. Sachova and Z. Sterbaček, Chem. Eng. J., 6, 195 (1973).
18. W. C. Clements, Chem. Eng. Sci., 24, 957 (1969).
19. A. S. Anderssen and E. T. White, Chem. Eng. Sci., 26, 1208 (1971).
20. M. L. Michelsen, Chem. Eng. J., 4, 171 (1972).
21. A. S. Anderssen and E. T. White, Can. J. Chem. Eng., 47, 288 (1969).
22. I. P. Sal'nikov and V. G. Ainshtein, Teor. Osn. Khim. Tekhnol., 10, 232 (1976).
23. G. Doetsch, Guide to the Application of Laplace and Z-Transforms, 2nd ed., Van Nostrand-Reinhold.
24. I. P. Sal'nikov, N. I. Gel'perin, V. G. Ainshtein, and R. A. Prakhova, in: The Mathematical Provision of Computers [in Russian], Part 2, MIKhMash, Moscow (1975), p. 28.
25. V. J. Law and R. V. Bailey, Chem. Eng. Sci., 18, 189 (1963).
26. K. Parami and T. R. Harris, Can. J. Chem. Eng., 53, 175 (1975).
27. A. H. Stroud and D. Secrest, Gaussian Quadrature Formulas, Prentice Hall, Englewood Cliffs, New Jersey (1966), p. 99.
28. L. A. Muzychenko, B. A. Veisbein, and S. Z. Kagan, Teor. Osn. Khim. Tekhnol., 6, 123 (1972).
29. M. M. Rozenberg, L. I. Kheifets, and M. B. Kats, Teor. Osn. Khim. Tekhnol., 4, 523 (1970).

NUMERICAL STUDY OF LAMINAR SWIRLED FLOW IN AN ANNULAR CHANNEL

V. V. Tret'yakov and V. I. Yagodkin

UDC 532.527

The effect of stream rotation on the velocity distribution in an annular channel is studied by the numerical method. The degrees of swirling corresponding to the initiation of stream separation are presented as functions of the Reynolds number for different values of the geometrical parameter of the channel.

I. It is known that the intensity of processes of heat and mass transfer in annular channels and pipes increases when swirled flows are used in them [1].

The attempts at an analytical solution of such problems are connected with certain simplifying assumptions. For example, the problem of the development of Poiseuille flow in a straight round pipe with stream rotation was solved in [2]. It was assumed that the changes in the flow caused by this rotation are small. This allowed the authors to solve the problem in a linear formulation. An approximate calculation of the development of swirled flow of a viscous incompressible liquid in a cylindrical pipe was the subject of [3], where assumptions were made that the radial velocity component and its derivative with respect to the radius are small, as well as the assumption that the axial velocity component differs little from its average value over the cross section.

Another approach to the solution of such problems is the numerical integration of the equations of motion of a viscous liquid. The velocity profiles of swirled flow in a round pipe were calculated in [4] using the method of [5]. It was found that the assumptions of [2] are not always satisfied.

Translated from Inzhenerno-Fizicheskii Zhurnal, Vol. 34, No. 2, pp. 273-280, February, 1978. Original article submitted December 20, 1976.

0022-0841/78/3402-0182$07.50

The numerical method of calculation of [5] will also be used in the present work.

II. The steady laminar flow of an incompressible liquid in a straight annular pipe in the presence of swirling of the stream at the inlet is analyzed. It is assumed that the flow is rotationally symmetrical, external mass forces are absent, and the density ρ and coefficient of dynamic viscosity μ are constants.

In a cylindrical coordinate system the Navier–Stokes equations for such flow have the form

$$\begin{gathered} v\frac{\partial u}{\partial r}+u\frac{\partial u}{\partial z}=-\frac{\partial p}{\partial z}+\frac{1}{\mathrm{Re}}\nabla^2 u, \\ v\frac{\partial v}{\partial r}+u\frac{\partial v}{\partial z}-\frac{w^2}{r}=-\frac{\partial p}{\partial r}+\frac{1}{\mathrm{Re}}\left(\nabla^2 v-\frac{v}{r^2}\right), \\ v\frac{\partial w}{\partial r}+u\frac{\partial w}{\partial z}+\frac{vw}{r}=\frac{1}{\mathrm{Re}}\left(\nabla^2 w-\frac{w}{r^2}\right), \\ \frac{\partial v}{\partial r}+\frac{v}{r}+\frac{\partial u}{\partial z}=0. \end{gathered} \tag{1}$$

Here u, v, and w are the axial, radial, and azimuthal velocity components, respectively, normalized to the average value u_{av} of the axial component over the radius; p is the pressure, normalized to ρu_{av}^2; $\mathrm{Re}=u_{av}/\nu$ is the Reynolds number, calculated over the width $a=R_2-R_1$ of the annular gap; ν is the coefficient of kinematic viscosity; R_2 and R_1 are the radii of the outer and inner cylinders, respectively; $\nabla^2\equiv\partial^2/\partial r^2+r^{-1}\partial/\partial r+\partial^2/\partial z^2$. All the linear dimensions are normalized to the characteristic dimension a of the problem.

For the flow under consideration the conditions of attachment must be satisfied at the walls:

$$u=v=w=0 \text{ at } r=R_1/a=R, \quad r=R_2/a=R+1. \tag{2}$$

The boundary conditions at the entrance cross section of the pipe are assigned by the profiles of the velocity components:

$$u=U_0(r), \quad v=0, \quad w=W_0(r) \text{ at } z=0. \tag{3}$$

As the boundary conditions at the exit cross section of the pipe we take

$$\frac{\partial u}{\partial z}=\frac{\partial v}{\partial z}=\frac{\partial w}{\partial z}+bw=0 \text{ at } z=L=L_c/a, \tag{4}$$

where L_c is the length of the channel; b is some positive number. The effect of the boundary conditions at the exit cross section can be judged from how much the solution changes with a change in b.

Boundary conditions will not be set up for the pressure, since later the pressure will be eliminated from the system (1) and only the velocity field in the channel will be found.

As the parameters on which the solution of the stated problem depends we take the following: the geometrical parameter R of the channel or the dimensionless radius of the inner cylinder, the Reynolds number Re, the dimensionless length L of the channel, and the profiles U_0 and W_0 of the axial and azimuthal velocities at the entrance.

A Poiseuille profile is chosen as the axial velocity profile U_0 in the present report and we consider the case when the radial variation of the azimuthal velocity component W_0 in the initial cross section $z=0$ within the channel takes place in accordance with a rigid-body law while the conditions of attachment are satisfied at the walls.

To characterize the quantitative relationship between the quantities u and w we introduce the quantity K, defined as

$$K(z)=\int_R^{R+1} w(r,\ z)\,dr\left[\int_R^{R+1} u(r,\ z)\,dr\right]^{-1}, \quad K_0=K(0).$$

The purpose of the report is the determination of the dependence of the solution of Eqs. (1) with the boundary conditions (2)–(4) on the parameters R, Re, and K_0 at values of L large enough that the solutions at a given length z_1 hardly vary with a further increase in L.

For future convenience we introduce the stream function ψ and the azimuthal component ω of the curl:

$$u = \frac{1}{r}\frac{\partial \psi}{\partial r}, \quad v = -\frac{1}{r}\frac{\partial \psi}{\partial r}, \quad \omega = \frac{\partial v}{\partial z} - \frac{\partial u}{\partial r}. \tag{5}$$

Using (5), the system (1) can be converted to the form

$$-\frac{\partial}{\partial z}\left(\frac{1}{r}\frac{\partial \psi}{\partial z}\right) - \frac{\partial}{\partial r}\left(\frac{1}{r}\frac{\partial \psi}{\partial r}\right) - \omega = 0,$$

$$\frac{\partial}{\partial z}\left(rw\frac{\partial \psi}{\partial r}\right) - \frac{\partial}{\partial r}\left(rw\frac{\partial \psi}{\partial z}\right) - \frac{\partial}{\partial z}\left[\frac{r^3}{\mathrm{Re}}\frac{\partial}{\partial z}\left(\frac{w}{r}\right)\right] - \frac{\partial}{\partial r}\left[\frac{r^3}{\mathrm{Re}}\frac{\partial}{\partial r}\left(\frac{w}{r}\right)\right] = 0, \tag{6}$$

$$r^2\left[\frac{\partial}{\partial z}\left(\frac{\omega}{r}\frac{\partial \psi}{\partial r}\right) - \frac{\partial}{\partial r}\left(\frac{\omega}{r}\frac{\partial \psi}{\partial z}\right)\right] - \frac{\partial}{\partial z}\left[\frac{r^3}{\mathrm{Re}}\frac{\partial}{\partial z}\left(\frac{\omega}{r}\right)\right] - \frac{\partial}{\partial r}\left[\frac{r^3}{\mathrm{Re}}\frac{\partial}{\partial r}\left(\frac{\omega}{r}\right)\right] - r\frac{\partial w^2}{\partial z} = 0.$$

Here the boundary conditions for the functions ψ, ω, and w, which follow from (2)-(5), have the form

$$\begin{gathered}
\psi = \int_R^r U_0(r)\, r dr \quad \text{at} \quad z = 0, \\
\psi = 0 \quad \text{at} \quad r = R, \\
\psi = \int_R^{R+1} U_0(r)\, r dr = 1 \quad \text{at} \quad r = R + 1, \\
\frac{\partial \psi}{\partial z} = 0 \quad \text{at} \quad z = L, \\
\omega = -\frac{\partial U_0}{\partial r} \quad \text{at} \quad z = 0, \\
\frac{\partial \omega}{\partial z} = 0 \quad \text{at} \quad z = L, \\
w = 0 \quad \text{at} \quad r = R, \quad r = R + 1, \\
\frac{\partial w}{\partial z} + bw = 0 \quad \text{at} \quad z = L.
\end{gathered} \tag{7}$$

The values of ω at the walls were replaced by their values at near-by points of the grid within the channel in accordance with the equation

$$(\omega/r)_P = [-3(\psi_{NP} - \psi_P)\Delta^{-2} - (\omega_{NP}/r_{NP})(0.5r_P^2 + r_P\Delta + 0.5\Delta^2)]\ [r_P^2 + 0.5r_P\Delta - \Delta^2/8]^{-1}. \tag{8}$$

Here φ_P is the value of the function φ at the wall; φ_{NP} is the value of the function φ in the layer nearest the wall; Δ is the radial step of the grid at the wall; r_P is the radius of the wall. Equation (8) was derived from assumptions concerning the possibility of a Taylor series expansion of the functions ψ and ω with respect to the parameter Δ near the wall using the second and third equations of the system (6).

III. The system of differential equations (6) was solved by the finite-difference method based on a conservative scheme with one-sided approximation of the convective terms, allowing for the direction of flow [5]. The calculations were made by the Gauss-Seidel iteration method. The iterations were stopped when the following conditions were satisfied:

$$\max_{i,j} |\psi_{ij}^n - \psi_{ij}^{n-1}| < 10^{-4}, \quad \max_{ij} \left| \left(\frac{\omega}{r}\right)_{ij}^n - \left(\frac{\omega}{r}\right)_{ij}^{n-1} \right| < 10^{-3},$$

$$\max_{ij} |(wr)_{ij}^n - (wr)_{ij}^{n-1}| < 10^{-3},$$

where n is the number of the iteration; φ_{ij} is the value of the function φ at node (i, j) of the grid.

The calculations, carried out on a 21 × 11 grid (21 lengthwise and 11 radially), uniform along the z axis and nonuniform radially (the law of radial variation of the step is parabolic) with Re = 10, R = 1, and L = 2.1, showed that the profiles of the azimuthal velocity, which is normalized to K_0, hardly depend on K_0. The results of calculations for K_0 = 6 are presented in Fig. 1a. A comparison of the profiles over the cross sections shows that in the axial direction the stream can be arbitrarily divided into two regions: an initial section directly adjacent to the entrance cross section, where a sharp change occurs in the azimuthal velocity profile from the

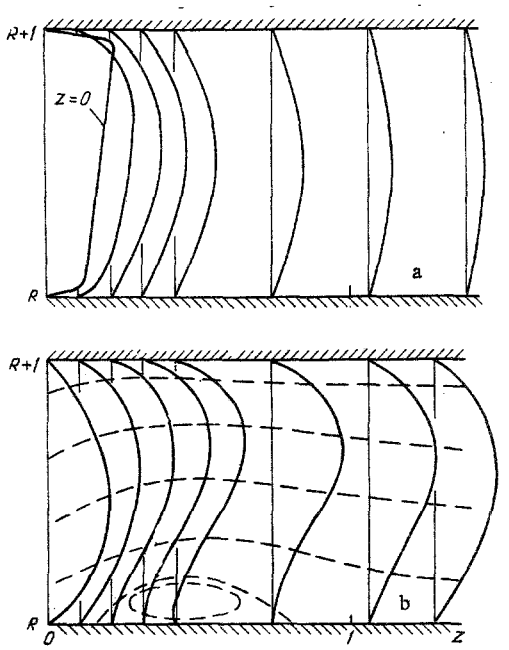

Fig. 1. Variation of profiles along channel axis: a) azimuthal velocity component w; b) axial component u (Re = 10, R = 1, L = 2.1, $K_0 = 6$).

assigned profile W_0 to its "natural" form, and a main section, where smooth variation of the generated "natural" profile occurs. The axial velocity profile varies smoothly from cross section to cross section along the length of the channel. In the process the streamlines first shift toward the outer wall owing to the action of centrifugal forces, while the velocity near the inner wall decreases somewhat. The dashed lines in Fig. 1b correspond to ψ = const. Then the streamlines again approach the inner wall owing to the attenuation of the azimuthal velocity along the length of the channel. The maximum of the axial velocity shifts in the same direction. With small values of K_0 these variations in axial velocity are small and the velocity profiles over the cross sections hardly differ. With an increase in swirling a zone of stream separation develops which occupies an ever larger region of flow as the swirling increases. The variation in the axial velocity component along the z axis is presented in Fig. 1b for $K_0 = 6$, at which stream separation from the inner wall already occurs. The point at which $(\partial u/\partial z)_{z_*} = 0$ or the axial component of the shear stress at the wall is $\tau_{wz} = \mathrm{Re}^{-1}(\partial u/\partial r)_{z_*} = 0$ was taken as the point of separation. The shear stress

$$|\tau_w| = \mathrm{Re}^{-1}[(\partial u/\partial r)^2 + (\partial w/\partial r)^2]^{1/2}$$

and its axial component τ_{wz} at the inner and outer walls as functions of the distance z along the axis for different values of the swirling K_0 are presented in Fig. 2. It is seen from the graphs that with nonseparation flow the contribution of the azimuthal component to the frictional stress is significant only in the initial section (the dashed and solid curves 1, corresponding to $K_0 = 1$, almost coincide at $z > 0.5$). It is also seen that when Re = 10 and R = 1 the quantity $K_0 = 5$ corresponds to a flow constant close to the separation value (the dashed curve 2 almost touches the abscissa), while with $K_0 = 10$ we obtain a region of separation corresponding to negative values of τ_{wz} (part of the dashed curve 3 is below the abscissa), with a zone of return currents like that shown in Fig. 1b for $K_0 = 6$ forming near the inner surface of the channel.

Analogous calculations were made for values of L greater than 2.1. The results proved to be similar. For L = 4, for example, the disagreements in the results of the calculation of K(z) for nonseparation flows at a length $z_1 = 1.5$ comprised fractions of a percent.

The influence of the grid on the solutions was studied. It was found that similar results are obtained for grids with a weak nonuniformity. For a uniform 21 × 21 grid, for example, the results practically coincide with those presented.

Systematic studies of the accuracy of the calculation scheme used showed that for Reynolds numbers in the range from 10 to 10^3 the solutions do not depend on the step Δ of the grid with acceptable accuracy when $\Delta \leq 10/\mathrm{Re}$. For $\Delta = 0.05$, for example, the differences in the results are 1-2%.

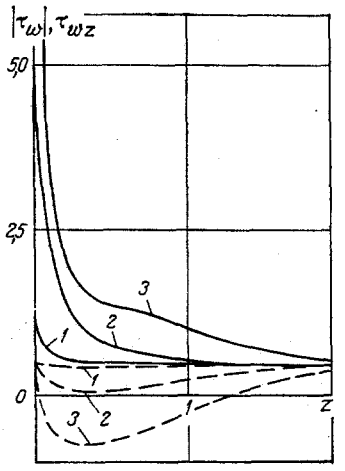

Fig. 2

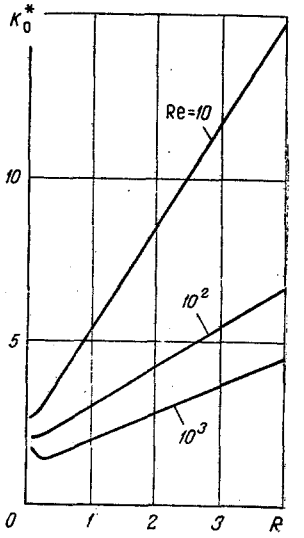

Fig. 3

Fig. 2. Variation of frictional stress at inner wall with different degrees of swirling: 1) $K_0 = 1$; 2) 5; 3) 10; solid curves) total shear stress ($|\tau_w|$); dashed curves) its axial component τ_{wz}.

Fig. 3. Dependence of "critical swirling" on geometrical parameter R and Reynolds number Re.

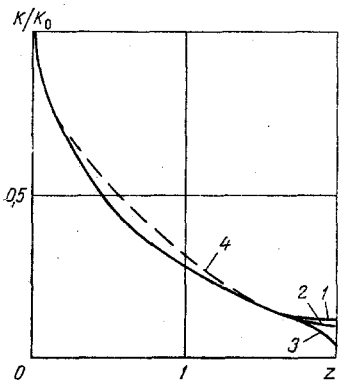

Fig. 4. Variation of relative stream swirling K/K_0 along channel length (Re = 10, R = 1, L = 2): 1, 2, 3) $K_0 = 1$; b = 0, b = 1, and $b = 10^2$, respectively, 4) $K_0 = 10$, b = 0.

Flow calculations were also made for channels with different parameters R in the range from 0.5 to 4.0 and with Reynolds numbers in the range from 10 to 10^3. The results did not vary qualitatively. The calculations showed that the degree of swirling K_0 at which separation first develops at the inner wall (we call it the "critical swirling" K_0^*) depends on both parameters R and Re. The calculations also showed that for a fixed R the point z_* at which separation develops moves away monotonically from the initial cross section as Re increases. Therefore, for Re > 10 the right-hand boundary conditions were set up at L = 10 or more and a nonuniform grid along the z axis was used.

IV. From the calculations in the ranges of variation of Re and R cited above we obtained the dependence $K_0^*(R, Re)$, which is presented in Fig. 3. It is seen from the graphs that for a fixed R separation sets in at larger values of K_0 with smaller Reynolds numbers, which is explained by the stabilizing action of the viscosity forces. It is also seen from the graphs that for each Reynolds number the stability of the flow against separation grows with an increase in R, since nonseparation flow must occur in the limiting case of $R \to \infty$. On the

other hand, with a decrease in R the profile of the axial velocity component becomes fuller in the vicinity of the inner wall, and in this case one could expect a strengthening of its stability against separation. One must keep in mind, however, than in this case along with the increase in the fullness of the profile near the inner wall there is also an increase in the centrifugal force in proportion to R^{-1}, the action of which is opposite to the influence of the profile. It is seen from Fig. 3 that K_0^* first declines slowly and then grows sharply as $R \to 0$, which should be expected from an estimate of the terms of the Navier–Stokes equations.

Actually, as $R \to 0$ the maximum in the profile of the axial velocity component approaches the inner wall, while the profile itself approaches the profile in a round pipe with the exception of some vicinity of the point r = 0. Thus, the natural scale of length along the radius near the inner wall will be $\delta = r_m - R$, where the axial velocity component varies from 0 to U_{max}. When $R \ll 1$ the quantity $\delta \ll L$, where L is the scale of length along the z axis. With allowance for the fact that $w \approx K_0^* u$, estimates in the equations of the system (1) near separation show that for each fixed Reynolds number, as $\delta \to 0$ there is a δ_1 such that $w \ll Re^{-1}\delta^{-2}$ occurs for any $\delta < \delta_1$, and consequently the order of magnitude of the pressure will be $p \approx Re^{-1}\delta^{-2}$. In this case the force action on the liquid in the radial direction will be determined by the projection of the pressure gradient $\partial p/\partial r$ and the centrifugal force. The latter must always remain in the equation, since it is the very cause of the stream separation from the inner wall. Then $w^2 r^{-1} \approx \partial p/\partial r$ or $K_0^* \approx \delta^{-1} Re^{-1/2}$. Thus, for small enough δ the quantity K_0^* grows with a decrease in δ. It must be noted, however, that the growth of K_0^* will actually be bounded as $R \to 0$, since stream separation can occur earlier due to instability relative to separation of the flow profile outside the δ layer. And this was observed in the numerical calculations. In this case for Re = 80 and R = 0.1 the quantity K_0^* proved to equal 1.84 and was close to its value calculated from the results of [4], although flow with an even velocity profile at the entrance was studied in the latter.

In conclusion, we note that calculations were also made with different boundary conditions (4) in the exit cross section. The quantity b was varied from 0 to 10^2. The variation of the swirling K/K_0 along the length of the channel for Re = 10 and R = 1 is shown in Fig. 4. The calculations showed that the attenuation of the swirling occurs in the same way for both nonseparation and separation flow when K_0 is close to K_0^*. The variation of the swirling along the length of the channel with developed separation ($K_0 = 10$) is shown by a dashed line in Fig. 4. It is also seen from the graphs that the influence of the form of the boundary conditions shows up only in the immediate vicinity of the exit cross section of the channel. The picture does not change qualitatively for other values of Re.

NOTATION

r, z	are the radial and axial coordinates;
u, v, w	are the axial, radial, and azimuthal velocity components;
R_1, R_2	are the radii of inner and outer cylinders;
L_c	is the length of channel;
a	is the characteristic dimension of the problem;
p	is the pressure;
ρ	is the density;
ν and μ	are the coefficients of kinematic and dynamic viscosity;
Re	is the Reynolds number;
ψ	is the stream function;
ω	is the azimuthal component of curl.

LITERATURE CITED

1. V. K. Shchukin, Heat Transfer and Hydrodynamics of Internal Streams in Mass Force Fields [in Russian], Mashinostroenie, Moscow (1970).
2. L. Talbot, J. Appl. Mech., 21, No. 1 (1954).
3. G. E. Sturov, in: Some Problems of the Study of the Vortex Effect and Its Industrial Application [in Russian], KAI, Kuibyshev (1974), p. 205.
4. M. F. Shnaiderman and A. I. Ershov, Inzh.-Fiz. Zh., 28, No. 4 (1975).
5. A. D. Gosman, V. M. Pan, A. C. Ranchel, D. B. Spalding, and M. Wolfshtein, Numerical Methods of Studying Viscous Fluid Flows [Russian translation], Mir, Moscow (1972).